Original Article

MOLECULAR METABOLISM

Control of hepatic gluconeogenesis by Argonaute2

Xin Yan [1,8], Zhen Wang [1,8], Christopher A. Bishop [1,6,8], Karolin Weitkunat [6], Xiao Feng [3], Marcel Tarbier [4], Jiankai Luo [3], Marc R. Friedländer [4], Ralph Burkhardt [5,7], Susanne Klaus [6], Thomas E. Willnow [1], Matthew N. Poy [1,2,*]

ABSTRACT

Objective: The liver performs a central role in regulating energy homeostasis by increasing glucose output during fasting. Recent studies on Argonaute2 (Ago2), a key RNA-binding protein mediating the microRNA pathway, have illustrated its role in adaptive mechanisms according to changes in metabolic demand. Here we sought to characterize the functional role of Ago2 in the liver in the maintenance of systemic glucose homeostasis.

Methods: We first analyzed Ago2 expression in mouse primary hepatocyte cultures after modulating extracellular glucose concentrations and in the presence of activators or inhibitors of glucokinase activity. We then characterized a conditional loss-of-function mouse model of *Ago2* in liver for alterations in systemic energy metabolism.

Results: Here we show that Ago2 expression in liver is directly correlated to extracellular glucose concentrations and that modulating glucokinase activity is adequate to affect hepatic Ago2 levels. Conditional deletion of *Ago2* in liver resulted in decreased fasting glucose levels in addition to reducing hepatic glucose production. Moreover, loss of *Ago2* promoted hepatic expression of *AMP-activated protein kinase* $\alpha 1$ (*AMPK*$\alpha 1$) by de-repressing its targeting by *miR-148a*, an abundant microRNA in the liver. Deletion of *Ago2* from hyperglycemic, obese, and insulin-resistant *Lep*$^{ob/ob}$ mice reduced both random and fasted blood glucose levels and body weight and improved insulin sensitivity.

Conclusions: These data illustrate a central role for Ago2 in the adaptive response of the liver to fasting. Ago2 mediates the suppression of *AMPK*$\alpha 1$ by *miR-148a*, thereby identifying a regulatory link between non-coding RNAs and a key stress regulator in the hepatocyte.

Keywords RNA-binding proteins; Energy homeostasis; Glucose metabolism; Metabolic stress; microRNAs; Cellular adaptation

1. INTRODUCTION

During fasting, the liver engages several mechanisms to facilitate hepatic glucose production. Central to this process are glycogenolysis and gluconeogenesis, which are strictly regulated at the transcriptional level to ensure expression of the enzymes catalyzing the rate limiting steps of these pathways [1]. These processes are also known to be impacted by post-translational modifications, as well as neuronal, nutrient, and hormonal signaling mechanisms [2,3]. Recent studies have now identified post-transcriptional regulators of liver function including non-coding RNAs and inhibition of abundant microRNAs in the liver including *miR-122*, *miR-103/107*, and *miR-148a* has been shown to affect energy metabolism, tumorigenesis, and insulin sensitivity [4–7].

Interestingly, liver-specific deletion of *miR-122* in mice reveals a complex phenotype including hepatosteatosis, increased inflammation, and spontaneous tumor formation [5,7]. This indicates that *miR-122* is unique in that other miRNAs co-expressed in the liver cannot functionally compensate for its absence. Previous studies have reported that *miR-122* is the most abundant sequence in the total miRNA pool, and the pronounced phenotype of the knockout mouse may also reflect this dominance over the expression profile [8]. This may also explain how *albumin*-Cre-mediated deletion of *Dicer* in mice recapitulated many of the phenotypic traits of the *miR-122*-knockout mice including the hepatosteatosis and hepatocarcinogenesis [9,10]. These results emphasizing altered lipid metabolism and tumorigenesis after abolishing *miR-122* and *Dicer* expression provide strong evidence for the miRNA pathway in playing a central role in regulating cellular

[1]Max Delbrück Center for Molecular Medicine, Robert Rössle Strasse 10, Berlin, Germany [2]John Hopkins University, All Children's Hospital, St. Petersburg, Florida, USA [3]Albrecht-Kossel-Institute for Neuroregeneration, Rostock University Medical Center, Gehlsheimer Straße 20, Rostock, Germany [4]Science for Life Laboratory, Department of Molecular Biosciences, The Wenner-Gren Institute, Stockholm University, 17121, Stockholm, Sweden [5]Institute of Laboratory Medicine, Clinical Chemistry and Molecular Diagnostics, University Hospital Leipzig, Liebigstrasse 27b, Leipzig, Germany [6]Department of Physiology of Energy Metabolism, German Institute of Human Nutrition Potsdam-Rehbrücke, Nuthetal, Germany [7]Institute of Clinical Chemistry and Laboratory Medicine, University Hospital Regensburg, Germany

[8] These authors contributed equally to this work.

*Corresponding author. Johns Hopkins All Children's Hospital, Johns Hopkins University School of Medicine, Department of Medicine, Division of Endocrinology, Diabetes and Metabolism, Institute for Fundamental Biomedical Research, 600 Sixth Avenue South, St. Petersburg, Florida, 33701, USA. Fax: +727 767 2821. E-mail: mpoy1@jhmi.edu (M.N. Poy).

Received August 14, 2018 • Revision received September 30, 2018 • Accepted October 4, 2018 • Available online 9 October 2018

https://doi.org/10.1016/j.molmet.2018.10.003

energy metabolism in the liver; however the full extent of its contribution remains to be elucidated.

The Argonaute family of proteins (Ago1-4) are essential regulators of microRNA function by mediating their interaction with target mRNAs and we recently showed loss of *Argonaute2* (*Ago2*), the highest expressed member of this family, in the pancreatic β-cell abolished compensatory proliferation during insulin resistance indicating that it serves in an adaptive capacity; however, it is unclear whether this function extends to other tissues essential to energy metabolism [11,12]. We also observed Ago2 expression in the β-cell was modulated in accordance to glucose metabolism providing further evidence that its function is directly linked to cellular energy homeostasis [13]. Moreover, the alterations in Ago2 expression in the β-cell were transient suggesting this form of post-transcriptional regulation may cooperate with other cellular mechanisms in managing the energy demands of the cell. In this study, we show Ago2 expression in the liver is modulated according to changes in extracellular glucose concentrations and conditional deletion in the hepatocyte diminished adaptive glucose production during fasting. Loss of Ago2 led to a concomitant increase in AMPKα expression indicating gene regulation by non-coding RNAs also overlaps with prominent signaling pathways managing cellular stress in the hepatocyte. Together these results identify Ago2 as an essential regulator of the fasting response of the liver and further reinforce the role of this RNA-binding protein and microRNAs in adaptive physiologic processes.

2. MATERIALS AND METHODS

2.1. Animals

Mice were maintained on a 12-hour light/dark cycle with ad libitum access to regular chow food, or ketogenic diet (cat. No. E15149-30, ssniff Spezialdiäten GmbH) in accordance with requirements established by Landesamt für Gesundheit und Soziales (LAGeSo). All experimental procedures were approved under protocols G 0357/10, G 0204/14, O 0405/09, and T 0436/08. *Albumin*-Cre-expressing mice on the C57BL/6 background were directly crossed to *Ago2*-floxed mice that were also on the C57BL/6 background (*Alb-Cre*, $Ago2^{flox/flox}$). The *Ago2* heterozygous mice carrying the *albumin*-Cre allele were then crossed to animals carrying the $Lep^{ob/ob}$ allele ($ob/Ago2^{Alb}$) (Jackson Labs). Results were consistent in both genders; however, data from female mice are not shown.

2.2. Analytic procedures

2.2.1. Quantification of metabolic parameters

Blood glucose levels were obtained with a One Touch glucometer (Bayer) and plasma insulin measurements were measured by ELISA (Crystal Chem, USA). Liver glycogen content was measured using the Glycogen Colorimetric Assay Kit (Biovision).

2.2.2. Antibodies for western blot analysis

The following primary antibodies were used for western blotting at 1:1000 dilution: Ago2 (MBL CM004-3), Ago1 (MBL RN028PW), Glucokinase (Abcam ab88056), β-Actin (Sigma A1978), GAPDH (Abcam ab8245), α-Tubulin (Sigma, T6557), Glucose-6-phosphatase (Abcam ab83690), Glycogen synthase (Cell Signaling, #3893), Insulin receptor (Cell Signaling, #3025), Akt2 (Cell Signaling, #2964), phospho-Akt2 (Ser474) (Cell Signaling, #8599), FoxO1 (Cell Signaling, #2880), phospho-FoxO1 (Cell Signaling, #9464), Acetyl-CoA Carboxylase (Cell Signaling, #3676), phospho-Acetyl-CoA Carboxylase (Cell Signaling, #11818), Fatty Acid Synthase (Cell Signaling, #3180), AMPKα (Cell Signaling, #2532), and phospho-AMPKα (Cell Signaling, #2535). Image densitometry of 16-bit TIF images for all western blots was performed using ImageJ.

2.2.3. Primary cell cultures

Primary hepatocytes were derived from livers of mice at age 10–12 weeks old and digested by collagenase, as previously described [14]. After centrifugation, tissue pellet was resuspended in DMEM (PAN Biotech) containing 4.5 g/L glucose supplemented with 10% FBS and 50 mg/mL penicillin and 100 mg/mL streptomycin for plating. Hepatocytes were cultured in 6-well plates coated with rat tail collagen I (Corning #453236). Media was changed 16 h later to starvation media containing 2.5 mM glucose supplemented with 0.5% v/v FBS and 50 mg/mL penicillin and 100 mg/ml streptomycin, until additional treatments were performed. 2-deoxyglucose (Sigma #D8375) and RO-28-1675 (ApexBio B1108) were solubilized in DMSO and added to the starvation media at the specified concentrations and cells were treated for 16 h before harvesting.

2.2.4. Isolation of mRNAs and miRNAs from ribonucleoprotein immunoprecipitation (RIP)

RIP experiments were performed as described previously [15,16]. In brief, the liver tissue from 16-hr fasted and random-fed C57BL/6 mice was lysed using an equal volume of lysis buffer (20 mM Hepes, 150 mM NaCl, 1 mM $CaCl_2$, 1 mM Mg Cl_2). After 5 min incubation on ice, lysates were frozen at −80 °C to enhance lysis. Samples were thawed on ice and spun for 15 min at 13,000 g and 4 °C to remove cell debris. Ago2 antibody (Wako cat. no. 018–22021) was incubated with Dynabeads Protein G (Invitrogen, 10004D) was on a rotating wheel for 4 h at 4 °C and beads were washed 5 times with wash buffer. Mouse IgG1 antibody was used as a negative control. Cleared lysates were incubated with beads overnight at 4 °C. Afterwards, beads were washed 5 times with elution buffer. RNA was extracted using the TRIzol reagent (Life Technologies). Incorporated mRNA or miRNA was quantified using qPCR and normalized by RNA from 10% input lysate.

2.2.5. Gene expression analysis

Total RNA was extracted using the TRIzol reagent (Invitrogen) and cDNA was synthesized using RevertAid First Strand cDNA synthesis kit (Fermentas). Quantitative real time PCR (qPCR) for microRNAs was performed using ABI microRNA assays and normalized to U6 expression (Applied Biosystems). Expression of mRNAs was assessed using gene-specific primers with FastStart SYBR Green PCR Master Mix (Roche) on a StepOne Real-Time PCR System (ThermoFisher). All primer sequences are available upon request. Luciferase assays were performed after cloning the mouse *AMPK* 3'UTR target site with the primers, 5′-TGGTAGCATAGCATAATGGG-3′ and 5′-CAACAGTTTATAGAGATATTCCTCAG-3′ into a pGL3 reporter vector (Pp-luc) (Promega). Co-transfection with miRNA mimics (Thermo Fisher Scientific) and a pRL-TK control vector (Rr-luc) was performed on HEK293 cells, harvested after 48 h, and assayed according to manufacturer's instructions (Promega). The control mimic pool was comprised of equimolar amounts of 8 independent miRNA mimics and the final transfected concentration was 200 nM.

2.2.6. Small RNA sequencing

Small RNA sequencing libraries were prepared using Illumina small RNA library preparation kits as described [16]. Small RNA fraction with a size range of 10–40 nucleotide (nt) were separated using flashPAGE Fractionator (Ambion) according to the manufacturer's instructions. The small RNA fractions were ligated sequentially at the 3′ and 5′ end

with synthetic RNA adapters, reverse transcribed and amplified using Illumina sequencing primers. Amplified libraries were purified by polyacrylamide gel electrophoresis (PAGE) according to the expected product size and libraries were sequenced for 50 cycles (Illumina Hi-seq 2000). The 3′ adapter sequences were removed using a custom Perl script and reads of length between 17 and 30 nt were mapped to known mouse pre-miRNA sequences deposited in miRBase (http://www.mirbase.org/) [17] without allowing any mismatch using soap1 and soap short [18], respectively.

2.3. Mouse phenotyping

Phenotyping analysis was performed in a 'blinded' manner; genotypes were unknown to the investigator during the experimentation and age of animals is stated in figure legends. All genotypes were present during all experiments and randomization was implemented to the extent that all animals were identified by number prior to analysis.

2.3.1. Tolerance tests

Glucose and pyruvate tolerance tests were performed following an overnight fast (16 h) and injected intraperitoneally with either glucose (2 g/kg body weight) or pyruvate (2 g/kg body weight in saline) as described [19]. Insulin tolerance tests were performed after same day fast (6 h) by injecting insulin (Sigma) intraperitoneally (0.75 U/kg body weight).

2.4. Blood analyses

Clinical chemistry parameters in mouse plasma were measured on an automated laboratory analyzer (Roche Cobas 8000). Plasma lipoproteins were isolated by sequential ultracentrifugation at density $<$1.006 g/mL (very-low-density lipoprotein [VLDL]), 1.006 $\leq$ d $\leq$ 1.063 g/mL (intermediate density lipoprotein, low-density lipoprotein [LDL]), and d $>$1.063 g/mL (high-density lipoprotein [HDL]) as described [20].

2.5. Statistical analysis

All results are expressed as mean $\pm$ standard error (SEM), and statistical analysis is summarized in Supplementary Table 3. Comparisons between data sets with two groups were evaluated using an unpaired Student's *t*-test. One-way and two-way repeated-measures ANOVA analysis has been performed using GraphPad Prism Software Version 7 for comparisons of three or more groups. Post hoc statistics were performed using Sidak's multiple comparison test. A *P*-value of less than or equal to 0.05 was considered statistically significant. The presented data met the assumptions of the statistical tests used. Normality and equal variances were tested using GraphPad Prism software. No statistical methods were used to pre-determine sample sizes, but our sample sizes are similar to those reported in previous publications [19].

3. RESULTS

3.1. Argonaute2 expression in liver is modulated according to glucose metabolism

Previous studies using the murine insulinoma-derived cell line MIN6 showed Ago2 expression to be regulated according to glucose metabolism [13]. We observed that expression of Ago2 in this pancreatic β-cell model increased in the presence of high glucose and hypothesized that its role in miRNA-mediated gene regulation was pertinent for the cellular adaptive response to increased glucose metabolism. Here we sought to test whether Ago2 functions in a similar capacity by also responding to changes in glucose metabolism in the liver. We incubated primary mouse hepatocytes in increasing concentrations of extracellular glucose and observed increased Ago2 and glucokinase (Gck) expression at 15 and 25 mM glucose levels in comparison to basal expression at 2.5 mM (Figure 1A). The increased expression of these genes was in direct contrast to the reduction in genes mediating gluconeogenesis including *glucose-6-phosphatase* (*G6pc*), *pyruvate carboxylase* (*Pc1*), and *phosphoenolpyruvate carboxykinase* (*Pepck*) (Figure 1B). We then tested whether pharmacological activation or inhibition of glucose metabolism impacts hepatic Ago2 levels by incubating primary mouse hepatocytes in the presence of 2-deoxyglucose (2-DG) or the glucokinase activator RO-28-1675. Inhibition of glucose metabolism with 2-DG abolished the increase in Ago2 expression in the presence of 25 mM glucose (Figure 1C,D) while treatment with RO-28-1675 resulted in increased levels of Ago2 (Figure 1E). To further test the correlation between Ago2 levels and cellular glucose metabolism in vivo, we next sacrificed wild-type C7BL/6 animals following a 16-hour overnight fast. Consistent with our *in vitro* observations, hepatic expression of Ago2 was observed decreased in fasted animals compared to levels in the random-fed cohort (Figure 1F). To further test whether this correlation was also consistent *in vivo* in a mouse model of hyperglycemia, we measured hepatic expression of Ago2 in leptin-deficient $Lep^{ob/ob}$ animals and observed higher levels compared to control littermates in the random-fed state (Figure 1G).

3.2. Conditional deletion of Argonaute2 in liver reduces fasting hepatic gluconeogenesis

To further test the role of Ago2 in hepatic glucose metabolism, we then generated a conditional, liver-specific, *Argonaute2* knockout mouse model by crossing the *Albumin*-Cre mouse line with an *Ago2* conditional allele (*Alb*-Cre, $Ago2^{flox/flox}$) (Figure 2A,B). To determine whether loss of hepatic Ago2 expression impacts systemic glucose homeostasis, we measured blood glucose levels at random steady-state and during an overnight 16-hour fast. In comparison to control littermates, *Albumin*-Cre, $Ago2^{flox/flox}$ (*Alb*-Cre, $Ago2^{flox/flox}$) mice exhibited decreased blood glucose levels only after the prolonged fast (Figure 2C). While no alterations were observed in body weight, insulin sensitivity and glucose tolerance (Figure 2D–F), blood glucose levels were significantly lower in Ago2-deficient mice after pyruvate challenge compared to wild-type control littermates indicating Ago2 contributes to hepatic glucose production (Figures 2G). To further test the function of Ago2 in gluconeogenesis, we placed *Alb*-Cre, $Ago2^{flox/flox}$ mice on a ketogenic diet for 30 days and exhibited decreased blood glucose levels in comparison to wild-type littermates (Figure 2H). Collectively, our results implicate an essential role for Ago2 in hepatic glucose production and indicate that Ago2/miRNA-mediated gene regulation facilitates adaptive physiologic processes.

In line with our earlier observations, fasting expression of *glucose-6-phosphatase* (*G6pc*), *phosphoenolpyruvate carboxykinase* (*Pepck*) and *pyruvate carboxylase* (*Pc1*) in the liver of *Alb*-Cre, $Ago2^{flox/flox}$ mice was decreased in comparison to levels in wild-type littermates (Figure 2I). In addition, we could confirm that glucose-6 phosphatase (G6Pase), glucokinase (Gck), and glycogen synthase2 (Gys2) were all reduced in livers of *Alb*-Cre, $Ago2^{flox/flox}$ mice compared to wild-type littermates by western blotting thereby further underlining the association between Ago2 and mediators of glucose metabolism (Figure 2J). No significant change was observed in fasting plasma insulin levels (Figure 2K); however, expression of the insulin receptor, and the phosphorylated levels of Akt2 (at Ser473), and FoxO1 (at Thr24) were decreased in *Alb*-Cre, $Ago2^{flox/flox}$ mice compared to

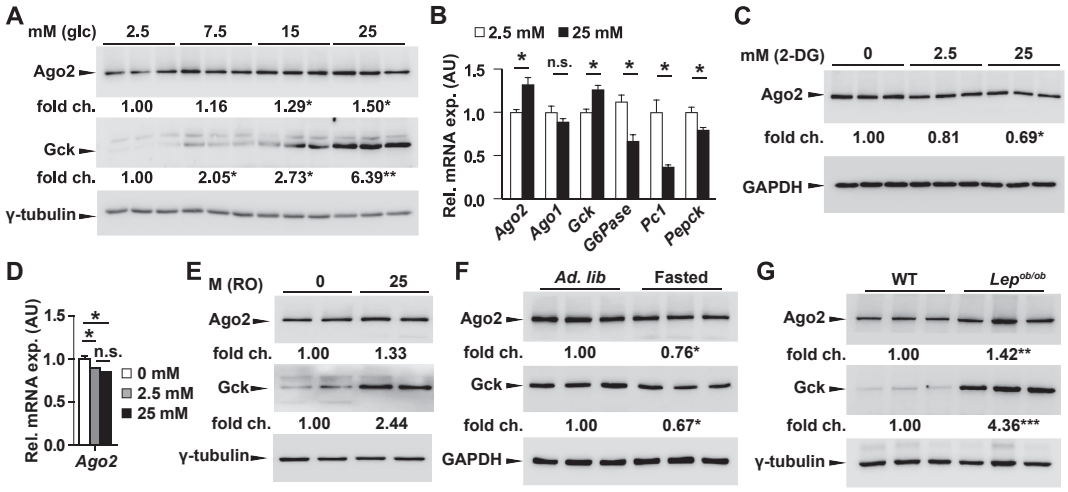

Figure 1: Argonaute2 in liver is modulated according to glucose metabolism. A, Western blotting analysis of Ago2 and glucokinase (Gck) in the isolated hepatocytes of 10-week-old WT mice that were treated ex vivo with 2.5 and 25 mM glucose (n = 3). **B**, Quantitative RT-PCR analysis of *Ago2*, *Ago1*, *Gck*, *G6pase*, *Pyruvate carboxylase* (*Pc1*), and *Phosphoenolpyruvate Caroxykinase* (*Pepck*) in the isolated hepatocytes of 10-week-old WT mice after treatment of 2.5 and 25 mM of glucose (n = 3 for both concentrations) for 48 h. **C, D**, Western blotting analysis of Ago2 in the isolated hepatocytes of 10-week-old WT mice after treatment with 0, 2.5, or 25 mM 2-deoxyglucose (2-DG) for 16 h (n = 3). **E**, Western blotting analysis of Ago2 in the isolated hepatocytes of 10-week-old WT mice after receiving 0 or 25 mM glucokinase activator (RO-28−1675) for 16 h (n = 2). **F**, Western blotting analysis of Ago2 and Gck from the liver of 10-week-old WT mice fasted for 16 h (n = 3). **G**, Western blotting analysis of Ago2 and Gck from the liver of 10-week-old *Lep*$^{ob/ob}$ mice and wild-type (WT) littermates (n = 3). Results are presented as mean ± SEM. *$P < 0.05$.

littermate controls indicating endogenous Ago2 impacts the insulin signaling cascade within the hepatocyte (Figure 2L, M).

3.3. Loss of Ago2 abolishes miRNA-mediated targeting of *AMPKα1*

To elucidate the molecular basis for the role of Ago2 in hepatic glucose control, we next sought to identify candidate target genes that are bound by Ago2:miRNA complexes. We first hypothesized that AMPKα may be subject to Ago2:miRNA-mediated gene regulation in the liver in light of its established role as a key mediator of hepatic glucose production and as a cellular stress sensor [21]. Indeed, the TargetScan algorithm identifies a putative binding site for *miR-148a* (also known as *miR-148a-3p*), an abundant miRNA present in the liver, within the 3' UTR of *AMPKa1* (also known as *PRKAA1* and in mouse as *Prkaa1*) (Supplementary Figure 1 and Supplementary Table 2) [22]. To first establish the direct interaction between Ago2, *miR-148a*, and the *AMPKα1* mRNA, we prepared liver lysates from wild-type C57BL/6 mice during random-fed and fasted states. Immunoprecipitation of Ago2 recovered increased levels of both *miR-148a* and *AMPKα1* mRNA from the lysates derived from random-fed mice compared to those from fasted mice indicating the interaction between these molecules is greater in the ad libitum state (Figure 3A). We further examined other abundant liver miRNAs in the Ago2 pull-down assay, including *miR-122*, *miR-152* and *miR-16*, and measured increased levels of these sequences indicating that in the random-fed state, additional miRNAs will also bind to Ago2 (Figure 3A).

We next tested whether hepatic expression of AMPK was altered in *Alb*-Cre, *Ago2*$^{flox/flox}$ mice to determine whether loss of Ago2 expression would disrupt potential miRNA-mediated regulation of *AMPKα1*. Western blotting analysis using an antibody raised to detect AMPKα revealed a marked increase in expression as well as its phosphorylated form (at threonine 172 (Thr172) in liver lysates from *Alb*-Cre, *Ago2*$^{flox/flox}$ mice in comparison to controls at age 10 weeks (Figure 3B). This increase in AMPKα expression is consistent with both disrupting miRNA-mediated gene regulation of a putative target as well as the decrease in fasting glucose levels observed in these Ago2-deficient mice. Moreover, we observed that the expression of *miR-148a* was decreased in the livers of *Alb*-Cre, *Ago2*$^{flox/flox}$ mice compared to littermate controls suggesting Ago2 may contribute to the stability of this sequence in the hepatocyte (Figure 3C). To confirm *AMPKα1* as a direct target of *miR-148a*, we over-expressed this miRNA in the presence of a luciferase reporter construct containing the region of the *AMPKα1* 3'-UTR that bears the putative binding site. Transfection of a *miR-148a* mimic resulted in the suppression of luciferase activity further suggesting this miRNA may directly target the *AMPKα1* gene (Figure 3D). Meanwhile, the transfection of mimics for which there is no binding site in the UTR fragment including *miR-27b*, *miR-124*, and *miR-128* did not affect luciferase reporter activity as expected and further supports the specificity of the interaction between *miR-148a* and the *AMPKα1* UTR. To further determine whether *AMPKα1* is directly targeted by *miR-148a*, we transfected miRNA mimics into primary hepatocytes derived from C57BL/6 mice and observed decreased protein and mRNA expression after increasing intracellular concentrations of *miR-148a* in comparison to the control pool of mimics (Figure 3E,F).

To address the physiologic relevance of the *miR-148a* targeting of *AMPKα1*, we next followed up on our previous results by quantifying hepatic AMPKα expression after fasting and during random-fed, steady state in hyperglycemic *Lep*$^{ob/ob}$ animals. Consistent with its role in miRNA-mediated, gene silencing, we observed that decreased expression of Ago2 in the livers of wild-type C57BL/6 mice after a 16-hour overnight fasting was accompanied by increased expression of AMPKα (Figure 3G). Conversely, increased hepatic expression of Ago2 in *Lep*$^{ob/ob}$ animals in the random-fed state is accompanied by decreased AMPKα expression (Figure 3H). Together these results illustrating the inverse relationship between Ago2 and AMPKα according to glycemic state provide further evidence for an important role for miRNA:Ago2-mediated gene regulation in the maintenance of systemic glucose homeostasis.

The effects on AMPKα expression in both the fasted and *Lep*$^{ob/ob}$ models also led to alterations in the phosphorylation of AMPKα (at

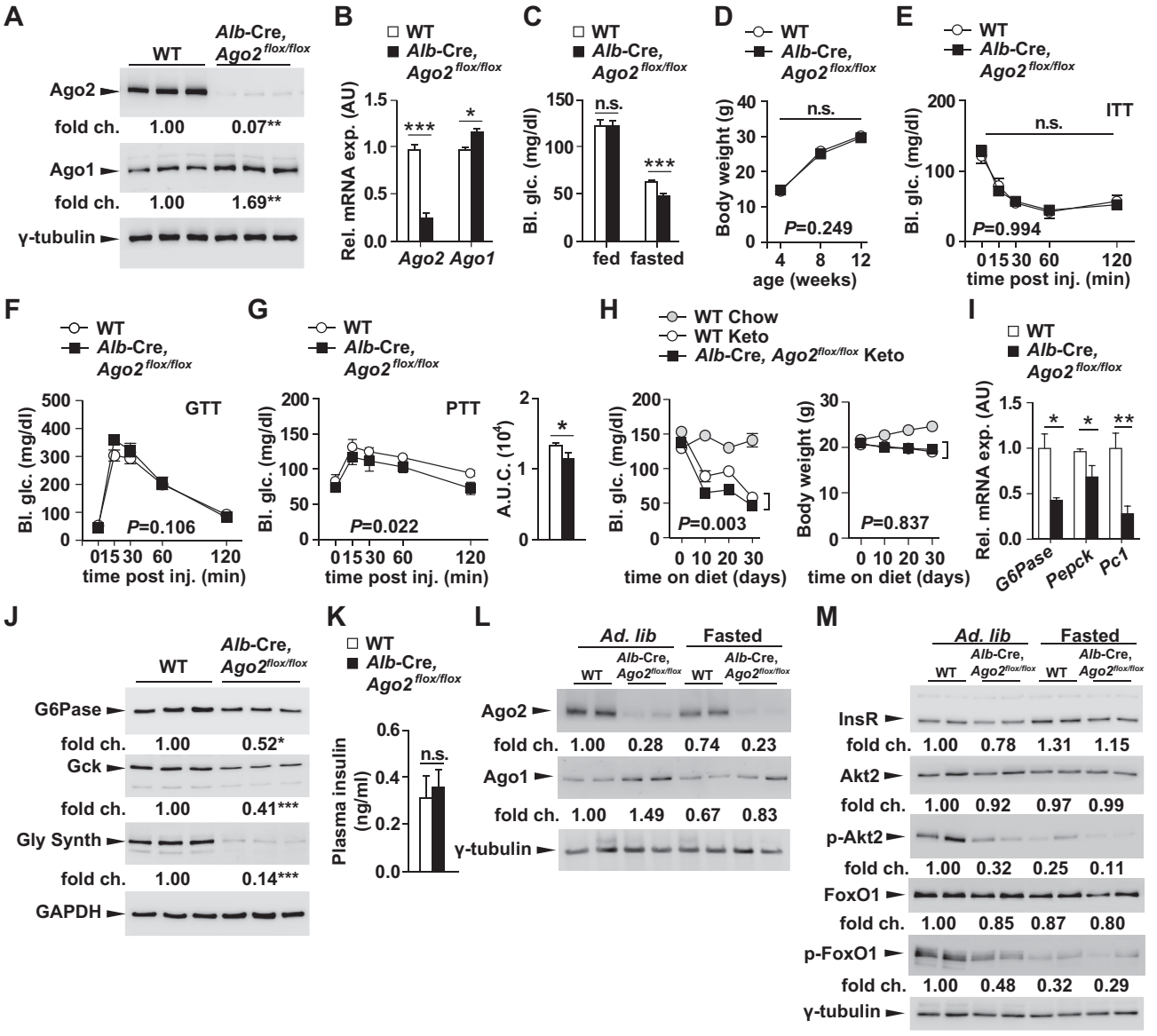

Figure 2: Loss of Argonaute2 in liver reduces hepatic gluconeogenesis. A, Western blotting analysis of Ago2 and Ago1 from liver of 8-week-old *Alb*-Cre, *Ago2*$^{flox/flox}$ mice and littermate controls (n = 3). **B**, qRT-PCR analysis of Ago2 and Ago1 from liver of 8-week-old *Alb*-Cre, *Ago2*$^{flox/flox}$ mice (n = 5) and littermate controls (n = 7). **C**, Random and fasting glucose measurements in 12-week-old *Alb*-Cre, *Ago2*$^{flox/flox}$ mice and littermate controls (n = 8–11). **D**, Body weight in male *Alb*-Cre, *Ago2*$^{flox/flox}$ mice (n = 13) and littermate controls (n = 14) from 4 to 12 weeks of age. **E**, Glucose measurements during an insulin tolerance test on 10-week old *Alb*-Cre, *Ago2*$^{flox/flox}$ mice (n = 5) and littermate controls (n = 6). **F**, Glucose measurements during a glucose tolerance test on 11-week old *Alb*-Cre, *Ago2*$^{flox/flox}$ mice (n = 7) and littermate controls (n = 6). **G**, Glucose measurements during a pyruvate tolerance test on 12-week old *Alb*-Cre, *Ago2*$^{flox/flox}$ mice (n = 5) and littermate controls (n = 6). **H**, Glucose measurements and body weight in the *Alb*-Cre, *Ago2*$^{flox/flox}$ mice (n = 8) and littermate controls (n = 4) on normal chow (Chow) or ketogenic diet (Keto, n = 8) for 30 days. **I**, qRT-PCR analysis of *G6Pase*, *Pepck* and *Pyruvate carboxylase* (*Pc1*) from liver of 8-week-old *Alb*-Cre, *Ago2*$^{flox/flox}$ mice (n = 5) and littermate controls after overnight fasting (n = 6). **J**, Western blotting analysis of glucose-6 phosphatase (G6Pase), glucokinase (Gck) and glycogen synthase (Gly synth) from liver of 8-week-old *Alb*-Cre, *Ago2*$^{flox/flox}$ mice and littermate controls after overnight fasting (n = 3). **K**, Plasma insulin measurements in 12-week old *Alb*-Cre, *Ago2*$^{flox/flox}$ mice (n = 7) and littermate controls after overnight fasting (n = 6). **L**, Western blotting analysis of Ago2 and Ago1 from liver of 8-week-old *Alb*-Cre, *Ago2*$^{flox/flox}$ mice and littermate controls during random-fed and overnight fasted states (16 h) (n = 2). **M**, Western blotting analysis of insulin receptor (InsR), phosphorylated Akt2 at Ser473 (p-Akt2), Akt2, phosphorylated FoxO1 at Thr24 (p-FoxO1) and FoxO1 from liver of 8-week-old *Alb*-Cre, *Ago2*$^{flox/flox}$ mice and littermate controls during random-fed and overnight fasted states (16 h) (n = 2). Results are presented as mean ± SEM. *$P < 0.05$, **$P < 0.01$ and ***$P < 0.001$.

Thr172) indicating concomitant changes in activity may also impact other mechanisms including lipid metabolism in addition to hepatic gluconeogenesis (Figure 3G,H). Acetyl-CoA carboxylase (ACC) is a prominent target of AMPKα and a key regulator of hepatic fatty acid metabolism and western blotting analysis of livers from *Alb*-Cre, *Ago2*$^{flox/flox}$ and littermate control mice revealed increased phosphorylation of ACC at serine 79 (Ser79) in the Ago2-deficient animals (Figure 3I). This was consistent with increased expression of total ACC expression, meanwhile no significant change was observed in fatty acid synthase (FAS) (Figure 3I). While *Alb*-Cre, *Ago2*$^{flox/flox}$ mice do not exhibit any alteration in total liver weight (Figure 3H), a mild increase in total hepatic triglyceride content was

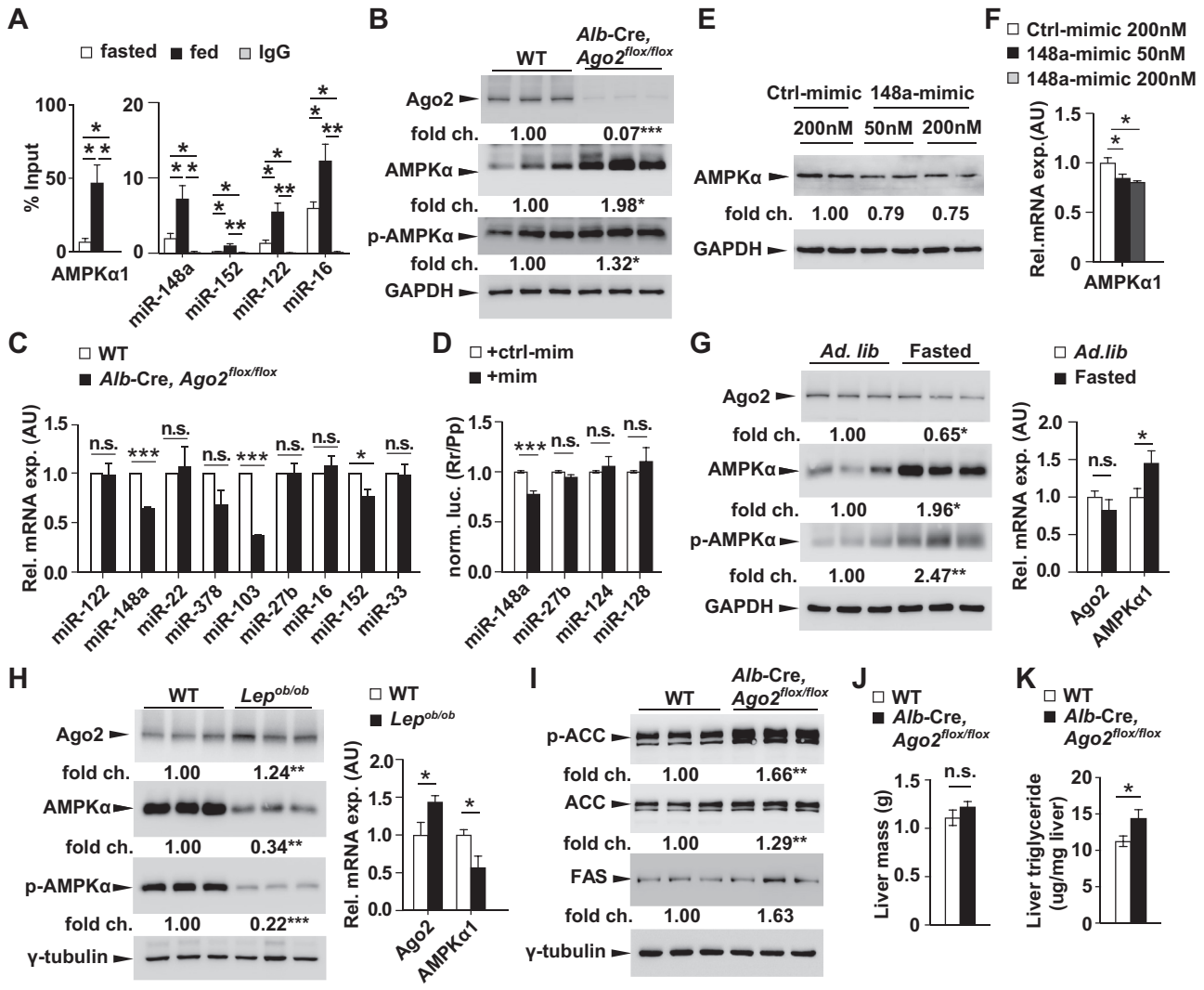

Figure 3: Loss of Ago2 abolishes miRNA-mediated targeting of AMPKα. **A**, Quantitative real-time PCR analysis of *AMPKα1* after immunopreciptation of Ago2 from liver tissue of C57BL/6 mice either fasted overnight for 16 h (white bar) or at random-fed (black bar) (n = 3–5). **B**, Western blotting analysis of Ago2, AMPKα and phosphorylated AMPKα at Thr172 (p-AMPKα) from liver of 8-week-old *Alb*-Cre, *Ago2*$^{flox/flox}$ mice and littermate controls after overnight fasting (n = 3). **C,** qRT-PCR analysis of microRNAs from liver of 10-week-old *Alb*-Cre, *Ago2*$^{flox/flox}$ mice (n = 7) and littermate controls after overnight fasting (n = 6). **D,** Luciferase assays in HEK cells testing direct targeting of AMPKα genes by *miR-148a* (148a-mimic), *miR-27b* (27b-mimic), *miR-124* (124-mimic), *miR-128* (128-mimic). **E**, **F**, Western blotting and qRT-PCR analysis of AMPKα after transfection of either a *miR-148a* mimic or a pool of control mimics into mouse primary hepatocytes. **G**, Western blotting analysis of Ago2, AMPKα and phosphorylated AMPKα at Thr172 (p-AMPKα) (n = 3) and qRT-PCR of *Ago2* and *AMPKα1* from the liver of 10-week-old WT mice during random-fed and overnight fasted conditions (16 h) (n = 5). **H**, Western blotting analysis of Ago2, AMPKα and phosphorylated AMPKα at Thr172 (p-AMPKα) (n = 3) and qRT-PCR of *Ago2* and *AMPKα1* from the liver of 10-week-old *Lep*$^{ob/ob}$ mice and wild-type (WT) littermates during random-fed and overnight fasted conditions (n = 6). **I**, Western blotting analysis of phosphorylated acetyl-CoA carboxylase at Ser79 (p-ACC), total ACC and fatty acid synthase (FAS) from liver of 8-week-old *Alb*-Cre, *Ago2*$^{flox/flox}$ mice and littermate controls after overnight fasting (n = 3). **J**, Quantification of total liver mass of *Alb*-Cre, *Ago2*$^{flox/flox}$ mice (n = 4) and littermate controls (n = 6). **K**, Quantification of liver triglyceride content of *Alb*-Cre, *Ago2*$^{flox/flox}$ mice (n = 7) and littermate controls after overnight fasting (n = 7). Results are presented as mean ± SEM. *$P < 0.05$, **$P < 0.01$ and ***$P < 0.001$.

measured in the livers of Ago2-deficient mice (Figure 3K). These results begin to indicate Ago2-mediated gene regulation can impact the pathways regulating both glucose and lipid metabolism.

3.4. Loss of *Ago2* improves glucose homeostasis in models of hyperglycemia, obesity and insulin resistance

To further test the in vivo relevance of Ago2 in the regulation of hepatic glucose production, we next crossed *Alb*-Cre, *Ago2*$^{flox/flox}$ mice onto the *Lep*$^{ob/ob}$ background (referred to as *ob/Ago2*^{Alb} mice) (Figure 4A). Interestingly, *ob/Ago2*^{Alb} mice exhibited lower body weight compared to their *Lep*$^{ob/ob}$ littermate controls due in large part to reduced fat mass (Figure 4B,C). Whereas no change in body weight was observed in *Alb*-Cre, *Ago2*$^{flox/flox}$ mice, loss of Ago2 in the context of physiologic stress elicited significant differences in metabolic parameters relevant to energy homeostasis. We next examined circulating glucose and insulin levels to see whether Ago2 would affect other signature features of the *Lep*$^{ob/ob}$ phenotype. Blood glucose and plasma insulin measurements were decreased in *ob/Ago2*^{Alb} mice in comparison to *Lep*$^{ob/ob}$ littermates at random-fed and fasting states further supporting our observations on the role of Ago2 in regulating hepatic gluconeogenesis and insulin sensitivity (Figure 4D–F). In addition, blood glucose levels were also lower in the Ago2-deficient animals

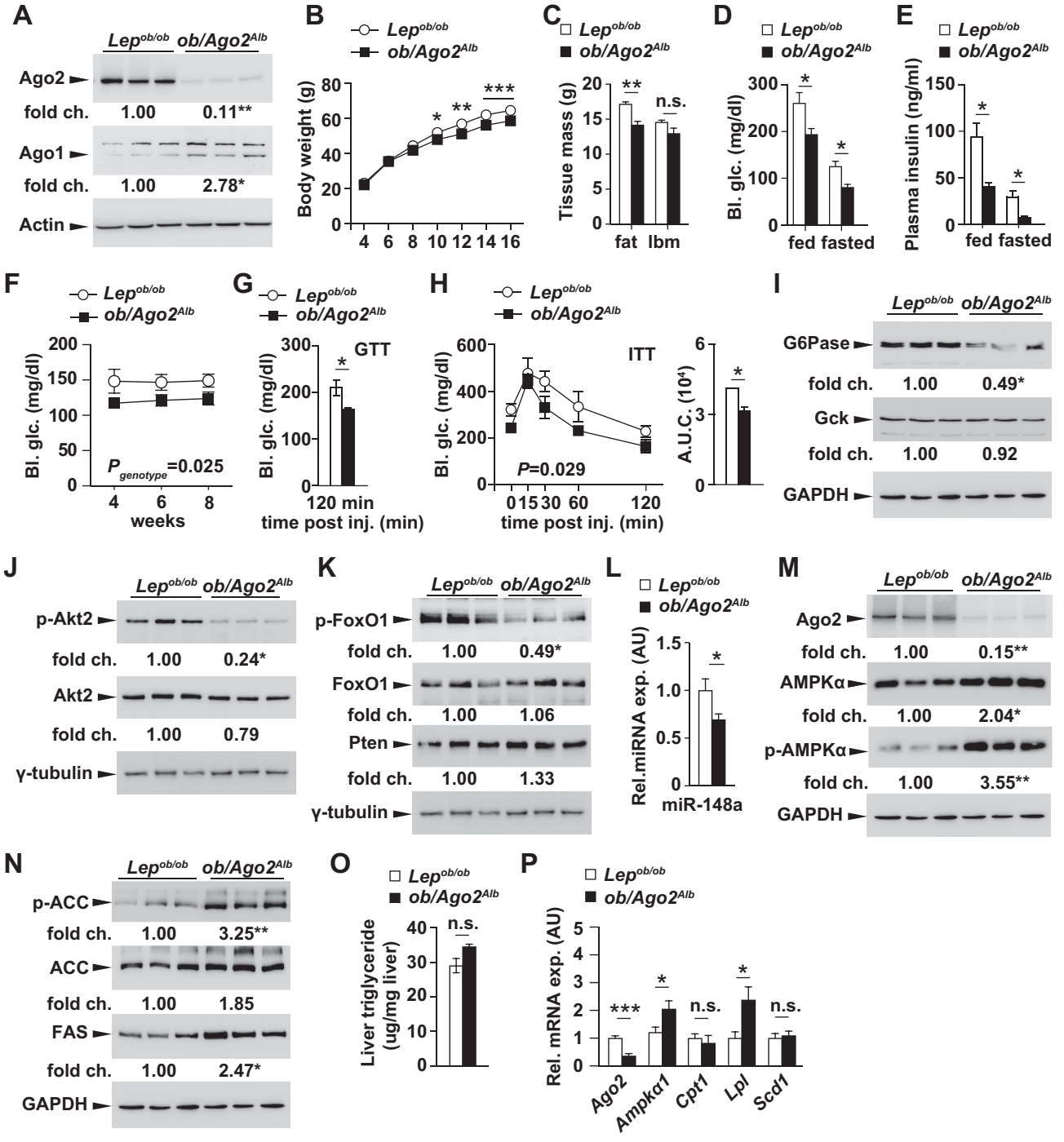

Figure 4: Loss of Ago2 improves glucose homeostasis during insulin resistance. A, Western blotting analysis of Ago2 and Ago1 from liver of 14-week-old *ob/Ago2^{Alb}* mice and control *Lep$^{ob/ob}$* littermates (n = 3). **B**, Body weight in male *ob/Ago2^{Alb}* mice (n = 6) and control *Lep$^{ob/ob}$* littermates (n = 9) from 4 to 16 weeks of age. **C**, Body composition in 10-week-old *ob/Ago2^{Alb}* mice (n = 3) and control *Lep$^{ob/ob}$* littermates (n = 3). **D**, Random and fasting glucose measurements in 14-week-old *ob/Ago2^{Alb}* mice (n = 4) and control *Lep$^{ob/ob}$* littermates (n = 6). **E**, Random and fasting plasma insulin measurements in 14-week-old *ob/Ago2^{Alb}* mice (n = 4) and control *Lep$^{ob/ob}$* littermates (n = 6). **F**, Random glucose measurements from 4-8-weeks old *ob/Ago2^{Alb}* mice (n = 6) and control *Lep$^{ob/ob}$* littermates (n = 3). **G**, Glucose measurements during a glucose tolerance test on 14-week old *ob/Ago2^{Alb}* mice (n = 3) and control *Lep$^{ob/ob}$* littermates (n = 3). **H**, Glucose measurements during an insulin tolerance test on 15-week old *ob/Ago2^{Alb}* mice (n = 3) and control *Lep$^{ob/ob}$* littermates (n = 3). **I**, Western blotting analysis of G6pase and Gck from liver of 14-week-old *ob/Ago2^{Alb}* mice and control *Lep$^{ob/ob}$* littermates after overnight fasting (n = 3). **J**, Western blotting analysis of phosphorylated Akt2 at Ser473 (p-Akt2) and Akt2 from liver of 14-week-old *ob/Ago2^{Alb}* mice (n = 3) and control *Lep$^{ob/ob}$* littermates after overnight fasting (n = 3). **K**, Western blotting analysis of phosphorylated FoxO1 at Thr24 (p-FoxO1), FoxO1 and Pten from liver of 14-week-old *ob/Ago2^{Alb}* mice and control *Lep$^{ob/ob}$* littermates after overnight fasting (n = 3). **L**, qRT-PCR analysis of *miR-148a* from liver of 14-week-old *ob/Ago2^{Alb}* mice and control *Lep$^{ob/ob}$* littermates (n = 6). **M**, Western blotting analysis of Ago2, AMPKα and phosphorylated AMPKα (p-AMPKα at Thr172) from liver of 14-week-old *ob/Ago2^{Alb}* mice and control *Lep$^{ob/ob}$* littermates after overnight fasting (n = 3). **N**, Western blotting analysis of phosphorylated acetyl-CoA carboxylase at Ser79 (p-ACC), ACC and fatty acid synthase (FAS) from liver of 14-week-old *ob/Ago2^{Alb}* mice and control *Lep$^{ob/ob}$* littermates after overnight fasting (n = 3). **O**, Liver triglyceride content of 20-week-old *ob/Ago2^{Alb}* mice (n = 4) and control *Lep$^{ob/ob}$* littermates (n = 6). **P**, Quantitative real-time PCR analysis of lipid metabolism genes from liver tissue of 14-week-old *ob/Ago2^{Alb}* mice after overnight fasting (n = 6) and control *Lep$^{ob/ob}$* littermates (n = 6). Results are presented as mean ± SEM. *$P < 0.05$, **$P < 0.01$ and ***$P < 0.001$.

during glucose and insulin tolerance tests indicating that specific targeting of Ago2 in the hepatocyte has extensive impact on systemic energy metabolism (Figure 4G,H). As we observed previously in *Alb*-Cre, $Ago2^{flox/flox}$ mice, hepatic G6Pase and Gck expression as well as phospho-Akt2 and phospho-FoxO1 were all similarly reduced in the livers of $ob/Ago2^{Alb}$ mice when compared to expression in $Lep^{ob/ob}$ controls (Figure 4I–K). Furthermore, we also confirmed on the $Lep^{ob/ob}$ background that loss of Ago2 incurs a reduction of *miR-148a* expression (Figure 4L). Likewise, the hepatic expression of AMPKα was increased in the livers of these animals, consistent with abolishing its regulation by the miRNA pathway (Figure 4M). Expression of both ACC and FAS were also observed increased in the livers of $ob/Ago2^{Alb}$ mice when compared to expression in littermate $Lep^{ob/ob}$ controls (Figure 4N). While the increased expression of lipogenic enzymes would be expected to promote hepatic lipid accumulation as in *Alb*-Cre, $Ago2^{flox/flox}$ mice, we observed no significant change in total liver triglyceride content in $ob/Ago2^{Alb}$ mice in comparison to $Lep^{ob/ob}$ littermates (Figure 4O). Furthermore, analysis of genes regulating fatty acid metabolism by quantitative RT-PCR only revealed a subtle increase in *lipoprotein lipase* (*Lpl*) (Figure 4P). While increased expression of hepatic Lpl would be consistent with an increase in circulating free fatty acids, we observed no change in plasma FFA levels in $ob/Ago2^{Alb}$ mice suggesting their uptake may also be elevated by peripheral tissues (Supplementary Table 1).

4. DISCUSSION

Numerous mechanisms at both the systemic and cellular level are present to aid in the adaptation to nutrient availability; however, the ongoing characterization of these pathways continues to expand the identification of molecules contributing to the regulation of energy metabolism [23]. By now, the microRNA pathway has been linked to virtually all cellular processes, yet a great deal still remains to be clarified regarding the functional role of these non-coding RNAs [24]. Here we report on the conditional loss of function mouse model of *Ago2* in the hepatocyte which illustrates a role for this RNA-binding protein and its associated miRNAs in maintaining fasting glucose levels. We identify *AMPKa1*, a mediator of hepatic glucose and lipid metabolism, as an intracellular target of *miR-148a* thereby directly linking non-coding RNAs to a key sensor of cellular stress in the liver.

As all living organisms depend on glucose for energy, mechanisms have evolved to manage cellular metabolism as demands fluctuate. Our observations here in the hepatocyte continue to allude to the broader role for the miRNA pathway as a central regulator of adaptive physiology that responds to changes in nutrient availability. One primary aspect of cell biology that remains unclear is how individual cells manage their intracellular metabolism to simultaneously maintain all of the ongoing functions performed by the cell. In the case of the pancreatic β-cell, we previously showed that loss of *Ago2* and *miR-375* in this cell type abolished compensatory proliferation in response to an increase in the demand for insulin during insulin resistance and hyperglycemia [12,25]. It is clear in this cellular context that, as the demand for insulin increases, the miRNA pathway acts to manage the balance between the energy requirements mandated for proliferation versus those that are necessary for exocytosis.

Here in the case of the hepatocyte, the reduction in glucose output during fasting again suggests that Ago2 and the microRNA pathway are central to maintaining a balance in cellular energy expenditure between multiple processes relying on the same energy pool. Our results showing reduced body weight and fat mass in the $ob/Ago2^{Alb}$ model in comparison to $Lep^{ob/ob}$ littermates clearly indicates deletion of hepatic *Ago2* impacts lipid metabolism in both the adipose and liver tissues. The reduction in adipose mass and in circulating triglycerides observed in $ob/Ago2^{Alb}$ animals is likely to be prompted by the overall improvement in glycemia, circulating insulin, and insulin sensitivity directly resulting from the loss of hepatic *Ago2* and the concomitant increase in AMPKα. Importantly, transient activation of AMPKα in liver was similarly shown to reduce fasting blood glucose levels and adipose mass, as well as increase liver triglyceride content suggesting the de-repression of *AMPK*α is a robust component of the *Ago2* knockout phenotype [26].

As hepatic AMPK expression is promoted during fasting, it is reasonable to speculate that Ago2 and its associated miRNAs are recruited to bind the 3'-UTR of targeted genes such as *AMPK*α*1* to halt translation as its functional demand fades such as in the post-prandial state; and when demand for expression has ceased for a prolonged period, the cell initiates the degradation of that mRNA perhaps as an 'energy saving' mechanism via the network of RNA-binding proteins that facilitate mRNA decay. In the context of human metabolism, cells such as beta cells or hepatocytes require mechanisms to handle sudden bouts of increased extracellular glucose and glucose influx during the day. Since these feeding events may be separated by a few hours or less, it is also plausible for cells to maintain and protect the integrity of essential transcripts perhaps by miRNA:Ago complexes to efficiently manage gene expression according to fluctuations in metabolic demand. At the cellular level, from an energy expenditure standpoint, this would be logical as opposed to constantly cycling between transcribing and decaying mRNAs in between feeding events.

While the precise mechanism remains unknown, this link between Ago2 and AMPKα may constitute a key switch between glucose and fatty acid metabolism. The decrease in plasma triglycerides may result from the increase in LPL expression that we measured in the livers of *Ago2*-deficient mice. While LPL expression is generally low in the liver, it has been shown to be up-regulated in conditions of low carbohydrate availability and increased expression of hepatic AMPK [26,27]. While Ago2 undoubtedly mediates the targeting of dozens of genes in the hepatocyte, it has not been established whether the up-regulation of genes such as LPL and ACC in our loss of function models is due to de-repression of miRNA targeting and should be subject to further investigation. Nonetheless, these results continue to delineate the complex network of prominent protein and non-coding RNA factors that maintain essential physiologic processes.

In light of these findings, future studies will eventually establish the full extent to which miRNA:Ago2-mediated gene regulation is in control of glucose and lipid homeostasis in the hepatocyte. As *miR-122* has long been known to be the most abundant miRNA in the liver (and therefore should occupy a large percent of Ago2 present in the hepatocyte), it should also be noted that there are significant areas of phenotypic overlap between our results presented here and the published studies on the *miR-122*-knockout mouse [5,7]. As shown in both loss of *miR-122* studies, *Alb*-Cre, $Ago2^{flox/flox}$ mice also exhibited reduced triglyceride levels in circulation; however we did not observe any alterations in circulating cholesterol as previously reported [5,7,28]. Additionally, we did not observe the development of spontaneous liver tumors in *Alb*-Cre, $Ago2^{flox/flox}$ mice through the age of 14 months in contrast to both papers on the *miR-122* knockout animals. While *miR-122* is likely to interact with a large part of the Ago2 pool, the most plausible explanation for these differences are the compensatory actions by either Ago1 or the collective loss of function of other miRNAs in our *Alb*-Cre, $Ago2^{flox/flox}$ model which offset or delay these phenotypic outcomes.

In addition to identifying additional Ago2-associated miRNAs and targets, several aspects of hepatic Ago2 function that should be further clarified include the identification of interacting proteins which affect

its function according to metabolic state. Previous studies have also shown that mitogenic signals may promote the recruitment of Ago2 to complex with other proteins suggesting additional proteins facilitate miRNA targeting [29]. Furthermore, recent studies have identified dozens of RNA-binding proteins that bind miRNAs and influence their expression thereby potentially increasing the complexity of studying miRNA-mediated gene targeting [30,31]. Lastly, it has also been shown that several phosphorylation sites are present on Ago2 and these sites have been shown to impact target gene suppression by miRNA [32] [33]. These recent studies have uncovered numerous intricacies of miRNA:Argonaute function and elucidating these dynamics within metabolic processes will continue to provide new insight into the pathways driving systemic energy homeostasis.

5. CONCLUSIONS

The ongoing examination of the miRNA pathway continues to clarify its functional association with virtually all cellular processes. In this study using genetic mouse models, we demonstrate that deletion of Ago2 results in lower systemic glucose levels during fasting and during the random-fed state in hyperglycemic $Lep^{ob/ob}$ mice further supporting this pathway as a mediator of adaptive cell physiology. Future studies aimed at miRNA:Ago-mediated gene regulation will continue the mapping of distinct networks that regulate energy metabolism and will facilitate the identification of mechanisms that may be pharmacologically targeted to reverse the onset of diabetes and obesity.

FUNDING

This work was funded by Johns Hopkins All Children's Hospital, the Helmholtz Gemeinschaft Metabolic Dysfunction Consortium, National Natural Science Foundation of China (81870587), the Chinese Scholarship Council (CSC No. 201306170014 to X.F.), and the European Research Council (ERC-2013-ADG-335692, to T.W.).

AVAILABILITY OF DATA AND MATERIAL

All primary data supporting the findings of this study are available on reasonable request.

AUTHOR'S CONTRIBUTIONS

X.Y., Z.W., C.B., K.W., X.F., M.T., J.L., M.F., R.B., S.K., T.W., and M.P. contributed to the conception and design of the study, and M.P wrote the manuscript. All authors approved the final version of this manuscript.

ACKNOWLEDGEMENTS

The authors would like to thank Liang Qiao, O. Halett, and N. Zampieri for helpful discussions and assistance in the conduct of this work.

CONFLICT OF INTEREST

The authors declare no competing interests.

APPENDIX A. SUPPLEMENTARY DATA

Supplementary data to this article can be found online at https://doi.org/10.1016/j.molmet.2018.10.003.

REFERENCES

[1] Petersen, M.C., Vatner, D.F., Shulman, G.I., 2017. Regulation of hepatic glucose metabolism in health and disease. Nature Reviews Endocrinology 13: 572–587. https://doi.org/10.1038/nrendo.2017.80.

[2] Shimazu, T., 1987. Neuronal regulation of hepatic glucose metabolism in mammals. Diabetes Metabolism Reviews 3:185–206.

[3] Lin, H.V., Accili, D., 2011. Hormonal regulation of hepatic glucose production in health and disease. Cell Metabolism 14:9–19. https://doi.org/10.1016/j.cmet.2011.06.003.

[4] Trajkovski, M., Hausser, J., Soutschek, J., Bhat, B., Akin, A., Zavolan, M., et al., 2011. MicroRNAs 103 and 107 regulate insulin sensitivity. Nature 474: 649–653. https://doi.org/10.1038/nature10112.

[5] Hsu, S.H., Wang, B., Kota, J., Yu, J., Costinean, S., Kutay, H., et al., 2012. Essential metabolic, anti-inflammatory, and anti-tumorigenic functions of miR-122 in liver. Journal of Clinical Investigation 122:2871–2883. https://doi.org/10.1172/JCI63539.

[6] Cheng, L., Zhu, Y., Han, H., Zhang, Q., Cui, K., Shen, H., et al., 2017. MicroRNA-148a deficiency promotes hepatic lipid metabolism and hepatocarcinogenesis in mice. Cell Death and Disease 8:e2916. https://doi.org/10.1038/cddis.2017.309.

[7] Tsai, W.C., Hsu, S.D., Hsu, C.S., Lai, T.C., Chen, S.J., Shen, R., et al., 2012. MicroRNA-122 plays a critical role in liver homeostasis and hepatocarcinogenesis. Journal of Clinical Investigation 122:2884–2897. https://doi.org/10.1172/JCI63455.

[8] Lagos-Quintana, M., Rauhut, R., Yalcin, A., Meyer, J., Lendeckel, W., Tuschl, T., 2002. Identification of tissue-specific microRNAs from mouse. Current Biology CB 12:735–739.

[9] Sekine, S., Ogawa, R., Ito, R., Hiraoka, N., McManus, M.T., Kanai, Y., et al., 2009. Disruption of Dicer1 induces dysregulated fetal gene expression and promotes hepatocarcinogenesis. Gastroenterology 136:2304–2315. https://doi.org/10.1053/j.gastro.2009.02.067 e1–4.

[10] Hand, N.J., Master, Z.R., Le Lay, J., Friedman, J.R., 2009. Hepatic function is preserved in the absence of mature microRNAs. Hepatology (Baltimore, Maryland) 49:618–626. https://doi.org/10.1002/hep.22656.

[11] Meister, G., 2013. Argonaute proteins: functional insights and emerging roles. Nature Reviews Genetics 14:447–459. https://doi.org/10.1038/nrg3462.

[12] Tattikota, S.G., Rathjen, T., McAnulty, S.J., Wessels, H.H., Akerman, I., van de Bunt, M., et al., 2014. Argonaute2 mediates compensatory expansion of the pancreatic β cell. Cell Metabolism 19:122–134. https://doi.org/10.1016/j.cmet.2013.11.015.

[13] Tattikota, S.G., Rathjen, T., Hausser, J., Khedkar, A., Kabra, U.D., Pandey, V., et al., 2015. miR-184 regulates pancreatic β-cell function according to glucose metabolism. Journal of Biological Chemistry 290:20284–20294. https://doi.org/10.1074/jbc.M115.658625.

[14] Li, W.-C., Ralphs, K.L., Tosh, D., 2010. Isolation and culture of adult mouse hepatocytes. Methods of Molecular Biology Clifton NJ 633:185–196. https://doi.org/10.1007/978-1-59745-019-5_13.

[15] Keene, J.D., Komisarow, J.M., Friedersdorf, M.B., 2006. RIP-Chip: the isolation and identification of mRNAs, microRNAs and protein components of ribonucleoprotein complexes from cell extracts. Nature Protocols 1:302–307. https://doi.org/10.1038/nprot.2006.47.

[16] Tattikota, S.G., Sury, M.D., Rathjen, T., Wessels, H.H., Pandey, A.K., You, X., et al., 2013. Argonaute2 regulates the pancreatic β-cell secretome. Molecular and Cellular Proteomics MCP 12:1214–1225. https://doi.org/10.1074/mcp.M112.024786.

[17] Kozomara, A., Griffiths-Jones, S., 2014. miRBase: annotating high confidence microRNAs using deep sequencing data. Nucleic Acids Research 42: D68–D73. https://doi.org/10.1093/nar/gkt1181.

[18] Li, R., Li, Y., Kristiansen, K., Wang, J., 2008. SOAP: short oligonucleotide alignment program. Bioinformation (Oxford, England) 24:713–714. https://doi.org/10.1093/bioinformatics/btn025.

[19] Rathjen, T., Yan, X., Kononenko, N.L., Ku, M.C., Song, K., Ferrarese, L., et al., 2017. Regulation of body weight and energy homeostasis by neuronal cell adhesion molecule 1. Nature Neuroscience 20:1096–1103. https://doi.org/10.1038/nn.4590.

[20] Burkhardt, R., Sündermann, S., Ludwig, D., Ceglarek, U., Holdt, L.M., Thiery, J., et al., 2011. Cosegregation of aortic root atherosclerosis and intermediate lipid phenotypes on chromosomes 2 and 8 in an intercross of C57BL/6 and BALBc/ByJ low-density lipoprotein receptor-/- mice. Arteriosclerosis Thrombosis and Vascular Biology 31:775–784. https://doi.org/10.1161/ATVBAHA.110.213843.

[21] Foretz, M., Viollet, B., 2011. Regulation of hepatic metabolism by AMPK. Journal of Hepatology 54:827–829. https://doi.org/10.1016/j.jhep.2010.09.014.

[22] Agarwal, V., Bell, G.W., Nam, J.-W., Bartel, D.P., 2015. Predicting effective microRNA target sites in mammalian mRNAs. eLife 4. https://doi.org/10.7554/eLife.05005.

[23] Soeters, M.R., Soeters, P.B., Schooneman, M.G., Houten, S.M., Romijn, J.A., 2012. Adaptive reciprocity of lipid and glucose metabolism in human short-term starvation. American Journal of Physiology Endocrinology and Metabolism 303:E1397–E1407. https://doi.org/10.1152/ajpendo.00397.2012.

[24] Bartel, D.P., 2018. Metazoan MicroRNAs. Cell 173:20–51. https://doi.org/10.1016/j.cell.2018.03.006.

[25] Poy, M.N., Hausser, J., Trajkovski, M., Braun, M., Collins, S., Rorsman, P., et al., 2009. miR-375 maintains normal pancreatic alpha- and beta-cell mass. Proceedings of the National Academy of Sciences of the United States of America 106:5813–5818. https://doi.org/10.1073/pnas.0810550106.

[26] Foretz, M., Ancellin, N., Andreelli, F., Saintillan, Y., Grondin, P., Kahn, A., et al., 2005. Short-term overexpression of a constitutively active form of AMP-activated protein kinase in the liver leads to mild hypoglycemia and fatty liver. Diabetes 54:1331–1339.

[27] Merkel, M., Weinstock, P.H., Chajek-Shaul, T., Radner, H., Yin, B., Breslow, J.L., et al., 1998. Lipoprotein lipase expression exclusively in liver. A mouse model for metabolism in the neonatal period and during cachexia. Journal of Clinical Investigation 102:893–901. https://doi.org/10.1172/JCI2912.

[28] Krützfeldt, J., Rajewsky, N., Braich, R., Rajeev, K.G., Tuschl, T., Manoharan, M., et al., 2005. Silencing of microRNAs in vivo with "antagomirs". Nature 438:685–689 https://doi.org/10.1038/nature04303.

[29] Olejniczak, S.H., La Rocca, G., Gruber, J.J., Thompson, C.B., 2013. Long-lived microRNA-Argonaute complexes in quiescent cells can be activated to regulate mitogenic responses. Proceedings of the National Academy of Sciences of the United States of America 110:157–162. https://doi.org/10.1073/pnas.1219958110.

[30] Nussbacher, J.K., Yeo, G.W., 2018. Systematic discovery of RNA binding proteins that regulate MicroRNA levels. Molecules and Cells 69:1005–1016.e7. https://doi.org/10.1016/j.molcel.2018.02.012.

[31] Treiber, T., Treiber, N., Plessmann, U., Harlander, S., Daiß, J.L., Eichner, N., et al., 2017. A compendium of RNA-binding proteins that regulate MicroRNA biogenesis. Molecules and Cells 66:270–284.e13. https://doi.org/10.1016/j.molcel.2017.03.014.

[32] Golden, R.J., Chen, B., Li, T., Braun, J., Manjunath, H., Chen, X., et al., 2017. An Argonaute phosphorylation cycle promotes microRNA-mediated silencing. Nature 542:197–202. https://doi.org/10.1038/nature21025.

[33] Quévillon Huberdeau, M., Zeitler, D.M., Hauptmann, J., Bruckmann, A., Fressigné, L., Danner, J., et al., 2017. Phosphorylation of Argonaute proteins affects mRNA binding and is essential for microRNA-guided gene silencing in vivo. The EMBO Journal 36:2088–2106. https://doi.org/10.15252/embj.201696386.

